Metal–Organic Frameworks

International Edition: DOI: 10.1002/anie.201602950
German Edition: DOI: 10.1002/ange.201602950

Hydrogen Storage and Selective, Reversible O_2 Adsorption in a Metal–Organic Framework with Open Chromium(II) Sites

*Eric D. Bloch, Wendy L. Queen, Matthew R. Hudson, Jarad A. Mason, Dianne J. Xiao, Leslie J. Murray, Roxana Flacau, Craig M. Brown, and Jeffrey R. Long**

Abstract: *A chromium(II)-based metal–organic framework $Cr_3[(Cr_4Cl)_3(BTT)_8]_2$ (Cr-BTT; BTT^{3-} = 1,3,5-benzenetristetrazolate), featuring coordinatively unsaturated, redox-active Cr^{2+} cation sites, was synthesized and investigated for potential applications in H_2 storage and O_2 production. Low-pressure H_2 adsorption and neutron powder diffraction experiments reveal moderately strong Cr–H_2 interactions, in line with results from previously reported M-BTT frameworks. Notably, gas adsorption measurements also reveal excellent O_2/N_2 selectivity with substantial O_2 reversibility at room temperature, based on selective electron transfer to form Cr^{III} superoxide moieties. Infrared spectroscopy and powder neutron diffraction experiments were used to confirm this mechanism of selective O_2 binding.*

Metal–organic frameworks have been rigorously studied for nearly two decades, and, although they are of interest for a wide range of potential applications related to ionic and electronic conductivity,[1] sensing,[2] catalysis,[3] and drug delivery,[4] they have been most extensively studied for gas storage[5] and separations.[6] Particularly promising for separations applications are classes of frameworks containing coordinatively unsaturated metal sites. Indeed, materials of this type have been shown to exhibit extraordinarily high capacities and adsorption selectivities for CO_2/N_2,[7] CO_2/H_2,[8] CO/H_2,[9] and paraffin/olefin separations,[10] among others. A particularly challenging and costly separation that is currently performed on an enormous scale (exceeding 100 Mtons/year[11]) is the separation of oxygen from nitrogen through cryogenic distillation. An efficient and selective adsorptive-based separation utilizing metal–organic frameworks could therefore offer tremendous energy and capital savings. However, few metal–organic frameworks exhibit the O_2 selectivity needed for such an application, presenting a design challenge that is compounded by the similar physical properties of O_2 and N_2, such as kinetic diameter, quadrupole moment, polarizability, and boiling point.[6d]

We have previously shown that by utilizing metal–organic frameworks containing coordinatively unsaturated, redox-active transition-metal cations, materials with high O_2/N_2 selectivities can be realized. These frameworks, $Cr_3(btc)_2$ (btc^{3-} = 1,3,5-benzentricarboxylate) and $Fe_2(dobdc)$ ($dobdc^{4-}$ = 2,5-dioxido-1,4-benzene-dicarboxylate), featuring accessible chromium(II) and iron(II) binding sites, respectively, displayed high O_2 adsorption capacities and excellent O_2/N_2 selectivities.[12] However, $Cr_3(btc)_2$ suffers from slow and incomplete O_2 desorption, whereas $Fe_2(dobdc)$ loses reversibility above 220 K. Still, these materials are currently the best metal–organic frameworks for O_2-selective separations and demonstrate the potential of redox-active metals for distinguishing O_2 from N_2. In addition to $Cr_3(btc)_2$ and $Fe_2(dobdc)$, the $M_3(btc)_2$ (M = Fe, Co, Ni, Cu, Zn, Mo, and Ru)[13] and $M_2(dobdc)$ (M = Mg, Mn, Co, Ni, Cu, Zn, and Cd)[14] framework types have been prepared with a variety of metal cations, though none of them have shown utility in the separation of O_2 from N_2. Metal–organic frameworks of the type $M_3[(M_4Cl)_3(BTT)_8]_2$ (M-BTT; M = Mn, Fe, Co, Cu, Cd; BTT^{3-} = 1,3,5-benzenetristetrazolate) have also been synthesized with a diversity of coordinatively unsaturated M^{2+} cations; however, none of these materials display selective O_2 adsorption and they have instead typically been studied as hydrogen-storage materials.[15] Herein, we describe the synthesis and characterization of a new member of the M-BTT family, Cr-BTT. Although this material displays only moderately strong Cr^{2+}–H_2 interactions, the electron-donating nature of the accessible chromium(II) centers endow it with excellent O_2/N_2 selectivity.

[*] Dr. E. D. Bloch, Dr. J. A. Mason, D. J. Xiao, Prof. Dr. J. R. Long
Department of Chemistry, University of California, Berkeley
Berkeley, CA 94720 (USA)
E-mail: jrlong@berkeley.edu
Prof. Dr. W. L. Queen
Institut des Sciences et Ingénierie Chimiques
École Polytechnique Fédérale de Lausanne (EPFL)
1051 Sion (Switzerland)
Dr. M. R. Hudson, Dr. C. M. Brown
Center for Neutron Research
National Institute of Standards and Technology
Gaithersburg, MD 20899 (USA)
Prof. Dr. L. J. Murray
Department of Chemistry, University of Florida
Gainesville, FL 32611 (USA)
Dr. R. Flacau
Canadian Neutron Beam Centre
National Research Council, Chalk River Laboratories
Chalk River, Ontario K0J 1P0 (Canada)
Dr. C. M. Brown
Department of Chemical Engineering
University of Delaware, Newark, DE 19716 (USA)
Prof. Dr. J. R. Long
Department of Chemical and Biomolecular Engineering
University of California, Berkeley and Materials Sciences Division
Lawrence Berkeley National Laboratory
Berkeley, CA (USA)
Supporting information and the ORCID identification number(s) for the author(s) of this article can be found under http://dx.doi.org/10.1002/anie.201602950.

The air-free reaction of anhydrous $CrCl_2$, $Cr(CO)_6$, H_3BTT, and trifluoromethanesulfonic acid in dimethylformamide (DMF) affords solvated $Cr_3[(Cr_4Cl)_3(BTT)_8]_2$ as a light-brown microcrystalline powder in high yield. X-ray powder diffraction data confirm that the material adopts the M-BTT structure type previously reported (Figure 1). The framework

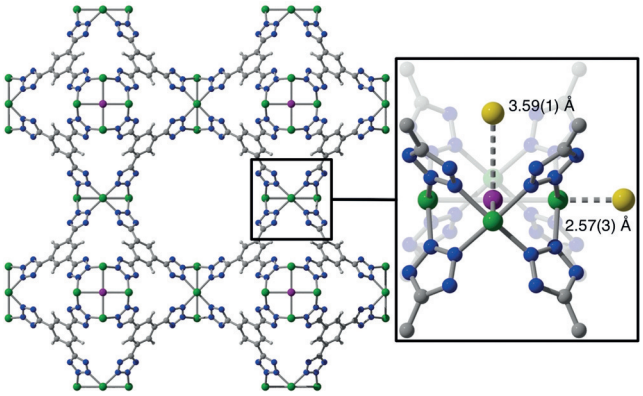

Figure 1. Left: A portion of the crystal structure of Cr-BTT as determined by neutron powder diffraction.[24] Atom colors: Cr dark green, Cl purple, C gray, N blue, H white. D_2 is shown as a single yellow sphere. Charge-balancing Cr atoms have been omitted for clarity. Right: Expanded portion of the structure of Cr-BTT dosed with D_2. At this loading, two binding sites are apparent with Cr–D_2 and Cl···D_2 distances of 2.57(3) and 3.59(1) Å, respectively.

was desolvated by first soaking in fresh DMF, followed by methanol exchange to remove coordinated DMF, and finally heating overnight at 150 °C under a dynamic vacuum to produce activated Cr-BTT. Nitrogen adsorption isotherms at 77 K reveal the framework to have Langmuir and BET surface areas of 2300 and 2030 $m^2 g^{-1}$, respectively. These values are in good agreement with those previously reported for other M-BTT frameworks, which display BET surface areas ranging from 1710 to 2100 $m^2 g^{-1}$, and the calculated surface area of 2293 $m^2 g^{-1}$ based on the crystal structure.[16]

Powder neutron diffraction data collected on the activated framework indicate the material crystallizes in the expected $Pm\bar{3}m$ space group with $a = 18.6688(3)$ Å. Although the Cr^{2+} ion has one of the largest ionic radii of the cations known to adopt the M-BTT structure type, only Cu-BTT has a smaller unit cell with $a = 18.595(7)$ Å.[15b] This somewhat unexpected observation stems from the fact that high-spin chromium(II) is a $3d^4$ metal center and is expected to display an axial elongation, akin to a Jahn–Teller distortion, and analogous to that observed for the $3d^9$ copper(II) centers in Cu-BTT. Indeed, the equatorial Cr–N distance of 2.078(2) Å is shorter than the M–N distance in all M-BTT frameworks, except for Cu-BTT (2.032(4) Å).

Given the combination of high surface area and accessible metal cation sites in Cr-BTT, coupled with the scarcity of reported hydrogen-storage studies for Cr^{II}-based metal–organic frameworks, we sought to investigate H_2 adsorption in Cr-BTT. Low-pressure adsorption isotherms measured at 77 and 87 K are presented in Figure 2. At 77 K, the H_2

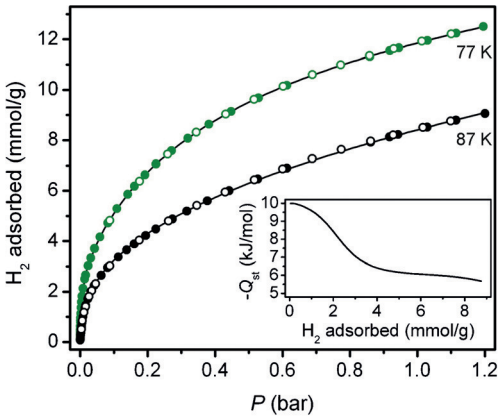

Figure 2. Excess H_2 adsorption isotherms at 77 K and 87 K for Cr-BTT after activation at 150 °C. Closed and open symbols represent adsorption and desorption, respectively. The solid lines correspond to dual-site Langmuir–Freundlich fits to each isotherm. Inset: Isosteric heat of H_2 adsorption plotted as a function of loading concentration.

isotherm is relatively steep, as expected for a metal–organic framework containing coordinatively unsaturated metal cation sites. Hydrogen uptake reaches a value of approximately 12 mmol g^{-1} (2.4 wt %) at 1 bar, which is very similar to the values reported for the Mn-, Fe-, and Cu-BTT frameworks (2.3, 2.3, and 2.4 wt %, respectively). Consistent with strong H_2 binding, the isosteric heat of H_2 adsorption (Q_{st}) plotted as a function of loading (Figure 2, inset) indicates a low-coverage adsorption enthalpy of −10.0 kJ mol^{-1}. This value is significantly greater in magnitude than that reported for the only other reported chromium(II) metal–organic framework, $Cr_3(btc)_2$ (−7.4 kJ mol^{-1}), which is a paddlewheel-based framework featuring strong Cr≡Cr quadruple bonds that decrease the Lewis acidity of the Cr^{2+} centers.[17] The low-coverage adsorption enthalpy in Cr-BTT is, however, comparable to the results previously reported for Mn-, Fe-, and Cu-BTT at −10.1, −11.9, and −9.5 kJ mol^{-1}, respectively.[18]

To further investigate the interaction of H_2 with Cr-BTT, we turned to powder neutron diffraction, which has previously proved valuable for structure elucidation in a variety of metal–organic frameworks.[19] Upon dosing two equivalents of D_2 per chromium site and cooling the sample to 10 K, two adsorption sites are apparent. Consistent with neutron diffraction studies on Mn-, Fe-, and Cu-BTT, the strongest two binding sites occur at the open Cr^{2+} cations, which bind D_2 with a Cr–D_2(centroid) distance of 2.57(3) Å, and above the μ_4-Cl^- ion, with a Cl···D_2(centroid) distance of 3.59(1) Å. The former value is longer than those previously reported for this structure type (2.17–2.47 Å) and is a result of the large ionic radius of Cr^{2+} and the significant axial elongation displayed by this $3d^4$ metal center.

The H_2 storage properties of Cr-BTT are in agreement with results published for the other members of the M-BTT family, while the strongly reducing nature of chromium(II) sets this framework apart and bodes particularly well for separation applications. To investigate the capability of Cr-BTT for selective oxygen binding, O_2 and N_2 adsorption

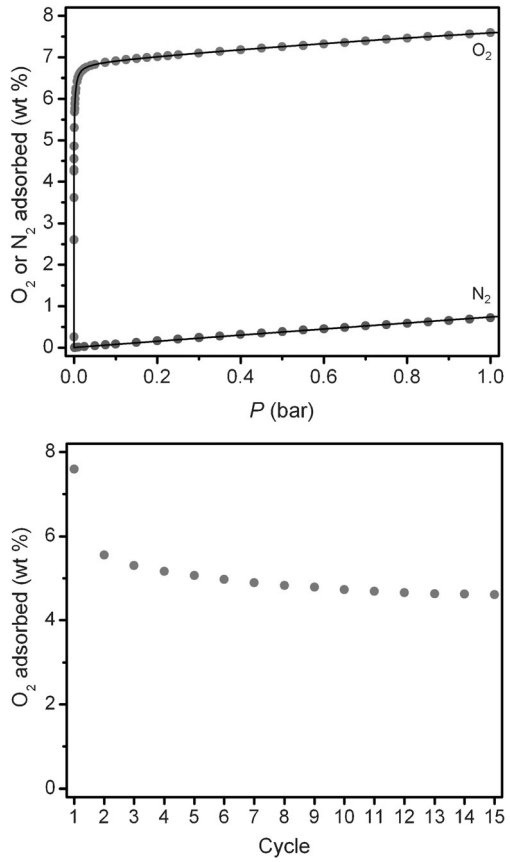

Figure 3. Top: Excess O_2 and N_2 adsorption isotherms collected for Cr-BTT at 298 K; the solid lines represent Langmuir–Freundlich fits to the data. Bottom: Uptake of O_2 at 200 mbar in Cr-BTT over 15 cycles at 298 K. Adsorption experiments were performed over 30 min and desorption was carried out by placing the sample under a dynamic vacuum at 423 K for 30 min.

isotherms were measured at 298 K (Figure 3). At this temperature, N_2 adsorption is minimal and climbs very gradually to just 0.69 wt % at 1 bar. The O_2 adsorption isotherm is extraordinarily steep, however, reaching 7.01 wt % at 0.20 bar before saturating at 7.59 wt % at 1 bar. This value falls short of the 11.3 wt % adsorption expected if every chromium(II) center in Cr-BTT were to bind an O_2 molecule, suggesting that a portion of the framework cations are somehow incapable of strongly binding oxygen. We note that this result is consistent with the plot of the isosteric heat of H_2 adsorption (Figure 2, inset), which displays an inflection point at 0.55 equiv of H_2 per framework metal center. Regardless, the room-temperature 1 bar adsorption capacity of 7.6 wt % is among the highest reported for a metal–organic framework, and Cr-BTT is surpassed only by Fe_2(dobdc) and Cr_3(btc), which exhibit capacities of 10 and 12 wt %, respectively.[12] Consistent with the higher O_2 capacity and steeper nature of the isotherm, Cr-BTT displays a dramatically larger O_2 adsorption enthalpy of approximately $-65\ kJ\,mol^{-1}$, as compared to $-15.3\ kJ\,mol^{-1}$ for N_2 (see the Supporting Information for additional isosteric heat calculation details).

We further employed ideal adsorbed solution theory (IAST) to predict how Cr-BTT would perform for the separation of an O_2/N_2 mixture. This method is useful for evaluating binary gas adsorption isotherms that cannot be conveniently and rapidly measured,[20] and has been widely established for a variety of gas mixtures in zeolites and metal–organic frameworks. The 298 K N_2 and O_2 adsorption isotherms were fit with single- and triple-site Langmuir–Freundlich models, respectively. For the separation of a 1:4 O_2:N_2 mixture at 298 K and 1 bar, Cr-BTT displays an IAST selectivity in excess of 2570. Significantly, this value corresponds to 99.3 % pure O_2 in the adsorbed phase at concentrations relevant to separation of air. To assess the utility of Cr-BTT for air separation, another important factor is the performance of this material under successive adsorption/desorption cycles. As shown in Figure 3 (bottom), Cr-BTT displays a moderate loss in capacity after the first adsorption/desorption cycle, showing a decreased uptake of 5.6 wt % on the second cycle. Capacity losses are then decreased over the next 13 cycles, and uptake appears to plateau near 4.6 wt % after 15 adsorption cycles. This represents, to the best of our knowledge, the highest stable cycling capacity for any porous material under mild conditions. Notably, this loss in capacity does not appear to arise from material degradation, as both the surface area and powder X-ray diffraction pattern remain unchanged after cycling.

The nature of the interaction between the chromium(II) centers of Cr-BTT and O_2 was probed by using infrared spectroscopy. A number of recent studies have been carried out on O_2 binding to molecular chromium(II) complexes for both end-on and side-on configurations.[21] These Cr^{3+}–O_2^- adducts feature O–O stretching frequencies ranging from 1070–1200 cm^{-1}, with the lower values typically corresponding to the side-on bound superoxide species.[22] For instance, the molecular complex exhibiting a metal coordination environment most similar to that found in Cr-BTT features a chromium(II) center coordinated to four equatorial N atoms of a cyclam ligand and an axial chloride anion.[23] This molecule was found to coordinate O_2 with the resulting Cr^{3+}–O_2^- complex displaying an O–O stretching frequency of 1170 cm^{-1}. It also represented the first crystallographically characterized end-on chromium(III) superoxo complex. Similarly, activated Cr-BTT displays two new infrared absorption bands upon exposure to O_2 (Figure S13). The isotopically sensitive O–O stretching frequency of 1193 cm^{-1} is suggestive of an end-on superoxide, while the Cr–O stretch at 769 cm^{-1} is further consistent with this interpretation.

To gain unambiguous insight into the nature of O_2 binding, we again turned to powder neutron diffraction experiments. A Rietveld refinement was performed against data collected for a sample of Cr-BTT that was dosed with approximately 1.5 equivalents of O_2 and subsequently cooled to 10 K. Similar to the adsorption of D_2, two adsorption sites are apparent for Cr-BTT at this loading. The highest occupancy site, with a refined occupancy of 0.83(2) O_2 molecules, is in the open chromium coordination site (Figure 4, left). Consistent with our interpretation of the infrared spectrum, the O_2 molecule binds in an end-on fashion with a Cr–O distance of 1.84(2) Å and a Cr-O-O angle of 129(2)°. This Cr–O distance is in good agreement with that reported for the only other crystallographically characterized

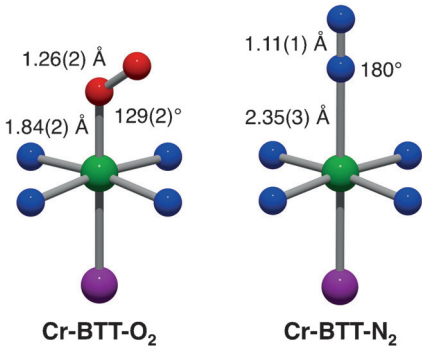

Figure 4. First coordination spheres for the chromium centers within O_2- and N_2-dosed Cr-BTT as determined from Rietveld analysis of powder neutron diffraction data. Atom colors: Cr dark green, Cl purple, O red, N blue. Values in parenthesis give the estimated standard deviation in the final digit of the number.

end-on chromium(III) superoxo complex (1.876(4) Å).[23] In contrast, the Cr-O-O angle here is significantly smaller than the 146.3(4)° reported for the molecular system, which is likely a result of the decreased steric bulk around the metal centers in Cr-BTT. Consistent with the formation of a superoxide, the O–O distance of 1.26(2) Å is elongated compared to that of free O_2 (1.2071(1) Å). Accordingly, the Cr–N and Cr–Cl distances of 2.064(3) and 2.569(20) Å in Cr-BTT decrease to 2.026(4) and 2.524(19) Å, respectively, upon oxidation of the metal center from chromium(II) to chromium(III). At this loading a secondary adsorption site 3.517(9) Å above the chloride ion with a refined occupancy of 0.25(2) is also apparent.

Powder neutron diffraction data were also collected on a sample of Cr-BTT dosed with N_2. At a loading of two N_2 molecules per metal, binding sites at both the chromium(II) center and above the chloride anion are occupied (Figure 4, right). In agreement with the weaker heat of adsorption as compared to O_2, N_2 coordinates in an end-on fashion at a much longer distance of Cr–N = 2.35(3) Å and with a Cr-N-N angle of 180°. The N–N distance is within error of the bond length in free N_2 (1.11(1) versus 1.0977(1) Å), which is expected given that high-spin chromium(II) is not expected to activate N_2. At the secondary binding site, the Cl···N distance of 3.62(3) is similar to the distances found for both D_2 and O_2 at this same site. Ultimately, the overall weak binding of N_2 to Cr-BTT as compared to O_2 endows this framework with excellent O_2/N_2 selectivity.

The foregoing results demonstrate the ability of Cr-BTT, a new metal–organic framework with open chromium(II) coordination sites, to selectively bind O_2 over N_2 through an electron-transfer mechanism. Furthermore, IAST calculations reveal a selectivity factor for O_2 in excess of 2500 at compositions relevant to air purification. Although cycling experiments indicate a moderate loss in O_2 capacity after the first adsorption/desorption cycle, a reversible capacity of at least 4.6 wt% is achieved at 298 K with rapid adsorption/desorption kinetics. Efforts are underway to improve both the loading capacity and recyclability of related materials.

Acknowledgements

This research was supported through the Center for Gas Separations Relevant to Clean Energy Technologies, an Energy Frontier Research Center funded by the U.S. Department of Energy, Office of Science, Office of Basic Energy Sciences under award DE-SC0001015. We thank Gerald K. Branch and Arkema for fellowship support of E.D.B., the NIST/NRC Fellowship program for support of M.R.H., the National Science Foundation for fellowship support of J.A.M. and D.J.X., and Dr. K. R. Meihaus for editorial assistance.

Keywords: air separation · chromium · metal–organic frameworks · neutron diffraction · superoxides

How to cite: *Angew. Chem. Int. Ed.* **2016**, *55*, 8605–8609
Angew. Chem. **2016**, *128*, 8747–8751

[1] a) M. Sadakiyo, T. Yamada, H. Kitagawa, *J. Am. Chem. Soc.* **2009**, *131*, 9906; b) Y. Kobayashi, B. Jacobs, M. D. Allendorf, J. R. Long, *Chem. Mater.* **2010**, *22*, 4120.

[2] a) B. Chen, L. Wang, F. Zapata, G. Qian, E. B. Lobkovsky, *J. Am. Chem. Soc.* **2008**, *130*, 6718; b) L. E. Kreno, K. Leong, O. K. Farha, M. Allendorf, R. P. Van Duyne, J. T. Hupp, *Chem. Rev.* **2012**, *112*, 1105.

[3] a) J. S. Seo, D. Whang, H. Lee, S. I. Jun, J. Oh, Y. J. Jeon, K. Kim, *Nature* **2000**, *404*, 982; b) C.-D. Wu, A. Hu, L. Zhang, W. Lin, *J. Am. Chem. Soc.* **2005**, *127*, 8940; c) S. Horike, M. Dinca, K. Tamaki, J. R. Long, *J. Am. Chem. Soc.* **2008**, *130*, 5854; d) L. Ma, C. Abney, W. Lin, *Chem. Soc. Rev.* **2009**, *38*, 1248; e) J. Lee, O. K. Farha, J. Roberts, K. A. Scheidt, S. T. Nguyen, J. T. Hupp, *Chem. Soc. Rev.* **2009**, *38*, 1450.

[4] a) P. Horcajada, T. Chalati, C. Serre, B. Gillet, C. Sebrie, T. Baati, J. F. Eubank, D. Heurtaux, P. Clayette, C. Kreuz, J.-S. Chang, Y. K. Hwang, V. Marsaud, P.-N. Bories, L. Cynober, S. Gil, G. Férey, P. Couvreur, R. Gref, *Nat. Mater.* **2010**, *9*, 172; b) J. Della Rocca, D. Liu, W. Lin, *Acc. Chem. Res.* **2011**, *44*, 957.

[5] a) M. Eddaoudi, J. Kim, N. Rosi, D. Vodak, J. Wachter, M. O'Keeffe, O. M. Yaghi, *Science* **2002**, *295*, 469; b) S. Kitagawa, R. Kitaura, S.-I. Noro, *Angew. Chem. Int. Ed.* **2004**, *43*, 2334; *Angew. Chem.* **2004**, *116*, 2388; c) R. Matsuda, R. Kitaura, S. Kitagawa, Y. Kubota, R. V. Belosludov, T. C. Kobayashi, H. Sakamoto, T. Chiba, M. Takata, Y. Kawazoe, Y. Mita, *Nature* **2005**, *436*, 238; d) A. R. Millward, O. M. Yaghi, *J. Am. Chem. Soc.* **2005**, *127*, 17998; e) H. Furukawa, M. A. Miller, O. M. Yaghi, *J. Mater. Chem.* **2007**, *17*, 3197; f) G. Férey, *Chem. Soc. Rev.* **2008**, *37*, 191; g) S. Ma, D. Sun, J. M. Simmons, C. D. Collier, D. Yuan, H.-C. Zhou, *J. Am. Chem. Soc.* **2008**, *130*, 1012; h) R. E. Morris, P. S. Wheatley, *Angew. Chem. Int. Ed.* **2008**, *47*, 4966; *Angew. Chem.* **2008**, *120*, 5044; i) P. L. Llewellyn, S. Bourrelly, C. Serre, A. Vimont, M. Daturi, L. Hamon, G. De Weireld, J.-S. Chang, D.-Y. Hong, Y. K. Hwang, S. H. Jhung, G. Férey, *Langmuir* **2008**, *24*, 7245; j) L. J. Murray, M. Dincă, J. R. Long, *Chem. Soc. Rev.* **2009**, *38*, 1294; k) B. Chen, S. Xiang, G. Qian, *Acc. Chem. Res.* **2010**, *43*, 1115.

[6] a) H. Hayashi, A. P. Côté, H. Furukawa, M. O'Keeffe, O. M. Yaghi, *Nat. Mater.* **2007**, *6*, 501; b) D. Britt, D. J. Tranchemontagne, O. M. Yaghi, *Proc. Natl. Acad. Sci. USA* **2008**, *105*, 11623; c) D. Britt, H. Furukawa, B. Wang, T. G. Glover, O. M. Yaghi, *Proc. Natl. Acad. Sci. USA* **2009**, *106*, 20637; d) J.-R. Li, R. J. Kuppler, H.-C. Zhou, *Chem. Soc. Rev.* **2009**, *38*, 1477.

[7] a) J. A. Mason, K. Sumida, Z. R. Herm, R. Krishna, J. R. Long, *Energy Environ. Sci.* **2011**, *4*, 3030; b) G. Férey, C. Serre, T. Devic, G. Maurin, H. Jobic, P. L. Llewellyn, G. De Weireld, A.

Vimont, M. Daturi, J.-S. Chang, *Chem. Soc. Rev.* **2011**, *40*, 550; c) J.-R. Li, J. Sculley, H.-C. Zhou, *Chem. Rev.* **2012**, *112*, 869.
[8] Z. R. Herm, J. A. Swisher, B. Smit, R. Krishna, J. R. Long, *J. Am. Chem. Soc.* **2011**, *133*, 5664.
[9] E. D. Bloch, M. R. Hudson, J. A. Mason, S. Chavan, V. Crocella, J. D. Howe, K. Lee, A. L. Dzubak, W. L. Queen, J. M. Zadrozny, S. J. Geier, L. C. Lion, L. Gagliardi, B. Smit, J. B. Neaton, S. Bordiga, C. M. Brown, J. R. Long, *J. Am. Chem. Soc.* **2014**, *136*, 10752.
[10] a) Z. Zhang, S. Xiang, B. Chen, *CrystEngComm* **2011**, *13*, 5983; b) E. D. Bloch, W. L. Queen, R. Krishna, J. M. Zadrozny, C. M. Brown, J. R. Long, *Science* **2012**, *335*, 1606; c) Y.-S. Bae, C. Y. Lee, K. C. Kim, O. K. Farha, P. Nickias, J. T. Hupp, S. T. Nguyen, R. Q. Snurr, *Angew. Chem. Int. Ed.* **2012**, *51*, 1857; *Angew. Chem.* **2012**, *124*, 1893; d) S. J. Geier, J. A. Mason, E. D. Bloch, W. L. Queen, M. R. Hudson, C. M. Brown, J. R. Long, *Chem. Sci.* **2013**, *4*, 2054.
[11] J. Emsley, *Oxygen, Nature's Building Blocks: An A – Z Guide to the Elements*, Oxford University Press, Oxford, **2001**.
[12] a) L. J. Murray, M. Dincă, J. Yano, S. Chavan, S. Bordiga, C. M. Brown, J. R. Long, *J. Am. Chem. Soc.* **2010**, *132*, 7856; b) E. D. Bloch, L. J. Murray, W. L. Queen, S. Chavan, S. N. Maximoff, J. P. Bigi, R. Krishna, V. K. Peterson, F. Grandjean, G. J. Long, B. Smit, S. Bordiga, C. M. Brown, J. R. Long, *J. Am. Chem. Soc.* **2011**, *133*, 14814.
[13] a) S. S.-Y. Chui, S. M.-F. Lo, J. P. H. Charmant, A. G. Orpen, I. D. Williams, *Science* **1999**, *283*, 1148; b) M. Kramer, U. Schwarz, S. Kaskel, *J. Mater. Chem.* **2006**, *16*, 2245; c) J. I. Feldblyum, M. Liu, D. W. Gidley, A. J. Matzger, *J. Am. Chem. Soc.* **2011**, *133*, 18257.
[14] a) N. L. Rosi, J. Kim, M. Eddaoudi, B. Chen, M. O'Keeffe, O. M. Yaghi, *J. Am. Chem. Soc.* **2005**, *127*, 1504; b) P. D. C. Dietzel, Y. Morita, R. Blom, H. Fjellvåg, *Angew. Chem. Int. Ed.* **2005**, *44*, 6354; *Angew. Chem.* **2005**, *117*, 6512; c) P. D. C. Dietzel, B. Panella, M. Hirscher, R. Blom, H. Fjellvåg, *Chem. Commun.* **2006**, 959; d) P. D. C. Dietzel, R. Blom, H. Fjellvåg, *Eur. J. Inorg. Chem.* **2008**, 3624; e) W. Zhou, H. Wu, T. Yildirim, *J. Am. Chem. Soc.* **2008**, *130*, 15268; f) S. R. Caskey, A. G. Wong-Foy, A. J. Matzger, *J. Am. Chem. Soc.* **2008**, *130*, 10870.
[15] a) M. Dincă, A. Dailly, Y. Liu, C. M. Brown, D. A. Neumann, J. R. Long, *J. Am. Chem. Soc.* **2006**, *128*, 16876; b) M. Dincă, W. S. Han, Y. Liu, A. Dailly, C. M. Brown, J. R. Long, *Angew. Chem. Int. Ed.* **2007**, *46*, 1419; *Angew. Chem.* **2007**, *119*, 1441; c) K. Sumida, S. Horike, S. S. Kaye, Z. R. Herm, W. L. Queen, C. M. Brown, F. Grandjean, G. J. Long, A. Dailly, J. R. Long, *Chem. Sci.* **2010**, *1*, 184; d) S. Biswas, M. Maes, A. Dhakshinamoorthy, M. Feyand, D. E. De Vos, H. Garcia, N. Stock, *J. Mater. Chem.* **2012**, *22*, 10200.
[16] T. Düren, F. Millange, G. Férey, K. S. Walton, R. Q. Snurr, *J. Phys. Chem. C* **2007**, *111*, 15350.
[17] K. Sumida, J. H. Her, M. Dincă, L. J. Murray, J. M. Schloss, C. J. Pierce, B. A. Thompson, S. A. FitzGerald, C. M. Brown, J. R. Long, *J. Phys. Chem. C* **2011**, *115*, 8414.
[18] K. Sumida, D. Stuck, L. Mino, J.-D. Chai, E. D. Bloch, O. Zavorotynska, L. J. Murray, M. Dincă, S. Chavan, S. Bordiga, M. Head-Gordon, J. R. Long, *J. Am. Chem. Soc.* **2013**, *135*, 1083.
[19] a) M. T. Kapelewski, S. J. Geier, M. R. Hudson, D. Stuk, J. A. Mason, J. N. Nelson, D. J. Xiao, Z. Hulvey, E. Gilmour, S. A. FitzGerald, M. Head-Gordon, C. M. Brown, J. R. Long, *J. Am. Chem. Soc.* **2014**, *136*, 12119; b) Z. Hulvey, B. Vlaisavljevich, J. A. Mason, E. Tsivion, T. P. Dougherty, E. D. Bloch, M. Head-Gordon, B. Smit, J. R. Long, C. M. Brown, *J. Am. Chem. Soc.* **2015**, *137*, 10816.
[20] J. A. Mason, T. M. McDonald, T.-H. Bae, J. E. Bachman, K. Sumida, J. J. Dutton, S. S. Kaye, J. R. Long, *J. Am. Chem. Soc.* **2015**, *137*, 4787.
[21] K. Qin, C. D. Incarvito, A. L. Rheingold, K. H. Theopold, *Angew. Chem. Int. Ed.* **2002**, *41*, 2333; *Angew. Chem.* **2002**, *114*, 2439.
[22] J. Cho, J. Woo, W. Nam, *J. Am. Chem. Soc.* **2012**, *134*, 11112.
[23] J. Cho, J. Woo, W. Nam, *J. Am. Chem. Soc.* **2010**, *132*, 5958.
[24] CCDC 1482071 – 1482078 contains the supplementary crystallographic data for this paper. These data are provided free of charge by The Cambridge Crystallographic Data Centre.

Received: March 24, 2016
Published online: June 1, 2016

